

# Numerical multidisciplinary optimization of aircraft with flight dynamic stability constraints

Proc IMechE Part G:  
*J Aerospace Engineering*  
2021, Vol. 235(1) 70–80  
© IMechE 2020  
Article reuse guidelines:  
[sagepub.com/journals-permissions](https://sagepub.com/journals-permissions)  
DOI: 10.1177/0954410020926659  
[journals.sagepub.com/home/pig](https://journals.sagepub.com/home/pig)



Jacek Mieloszyk

## Abstract

Classical approach to conceptual and preliminary design in aerospace sciences reaches limits. To go further and achieve better, competitive results' use of optimization methods becomes mandatory. The trend is clearly visible in professional software for simulations equipped with optimization tools, which was not standard just decade ago. Many examples of multidisciplinary optimization were shown, especially with coupled aerodynamics and structure analyses, but only few of them consider dynamic stability effects in the conceptual and preliminary design. The article shows successful example of multidisciplinary design and optimization of Vertical Takeoff and Landing aircraft, which includes coupling of aerodynamics, mass analyses and innovative approach of constraints from flight dynamic stability. Presented optimization framework revealed potential for more efficient conceptual and preliminary design with the result of known dynamic stability characteristics of the aircraft. Obtaining the dynamic stability characteristics is not common on the early stages of the design yet crucial for the aircraft flight performance.

## Keywords

Flight dynamics constraints, MDO, numerical optimization, Particle Swarm Optimization, VTOL

Date received: 1 January 2020; accepted: 18 April 2020

## Introduction

The object of optimization is a multipurpose Vertical Takeoff and Landing (VTOL) unmanned aircraft. There is a demand on the market for such type of aircrafts, which are relatively cheap to manufacture and use, compared to typical manned aircraft. Furthermore, unmanned aircrafts offer possibility to conduct missions, which could be dull, dirty or dangerous for humans. In particular, VTOL type of aircraft, which is a hybrid of airplane and multicopter, combines advantages of the two, which is a possibility to take off and land without runway and travel for long distances. The advantages come at a price of complexity of the system. The aircraft has to satisfy number of constraints and performance requirements. Although, it is conceptual design phase to obtain reliable results for such a complicated object as VTOL aircraft, it has to be sufficiently well modelled. The optimization includes analyses of aerodynamics, mass estimation and flight dynamics constraints. Many examples of multidisciplinary optimization can be shown, especially with coupled aerodynamics and structure analyses. Starting from airliners optimization<sup>1,2</sup> through supersonic aircrafts<sup>3</sup> and ending

up even with morphing structures.<sup>4,5</sup> Although variety of examples is very wide, only a few of design examples consider dynamic stability effects in the conceptual and preliminary design. In most cases, the designs are limited to longitudinal, or lateral stability modes<sup>3,6,7</sup> or to simplified configuration like flying wing.<sup>8,9</sup> Flight dynamics analyses during the conceptual design are rarely done. In most cases, only requirement for static stability is checked, and dynamic stability analyses are done at the end of the conceptual design<sup>10,11</sup> to check if the design is feasible and flyable.<sup>12</sup> It may be sound approach for aircrafts with classical configuration, which are well known, and there are many similar, representative, operating aircrafts, which were built for the particular purpose. This statement will not hold for innovative configurations, such as VTOL aircraft. The reason for such a

---

Institute of Aeronautics and Applied Mechanics, Warsaw University of Technology, Warsaw, Poland

### Corresponding author:

Jacek Mieloszyk, Warsaw University of Technology, Nowowiejska 24, 00-665 Warsaw, Poland.

Email: [jmieloszyk@meil.pw.edu.pl](mailto:jmieloszyk@meil.pw.edu.pl)

general approach is requirement for dynamic stability data, which are aerodynamic and mass characteristics data. Therefore, aircraft's aerodynamic configuration and at least main structure components have to be defined and considered. Details about basis of the new optimization approach with the dynamic stability constraints framework can be found in Mieloszyk and Goetzendorf-Grabowski.<sup>13</sup>

The design has basic utility requirements for payload weight and size, which force strict requirements for power needed for vertical flight and for size and masses of the vertical propulsion system. Due to flight law regulations, it was also assumed that the total weight for flight cannot exceed 25 kg. Utilizing these assumptions, mandatory technical requirements were defined. The initial aircraft configuration is shown in Figure 1.

### Analyses used in the optimization

As stated in the introduction to obtain reliable results, simple but accurate model of the problem has to be formulated. For that purpose, different simulations were used, which are described in the subsequent chapters.

#### Aerodynamic analyses

The aerodynamic analyses were done utilizing Panukl software,<sup>14,15</sup> which was coupled with a two-dimensional viscous panel method in Xfoil software for airfoil analyses.<sup>16</sup> All aerodynamic values of forces and moments were taken directly from the 3D panel method except the drag force. The drag was corrected according to equation (1). The total drag contained a few components which included pressure drag from 3D panel method for the whole aircraft model, friction part of drag of all the wing surfaces and the friction part of fuselage drag. For the wing-type surfaces like the main wing, horizontal stabilizer and vertical stabilizers MAC were calculated. For the MAC, for the particular wing surface, two-dimensional viscous analyses were done to obtain friction part of the drag. Additionally, constant friction part of the drag for

fuselage was estimated based on analytical formula from flight mechanics<sup>17</sup>

$$D_{total} = D_{3D\_panel\_method} + D_{f\_wings} + D_{f\_fuselage} \quad (1)$$

#### Mass estimation analyses

To conduct dynamic stability analyses, mass properties were needed. Total mass consisted of the following components: wing mass, fuselage mass, tail booms masses, payload mass, avionics mass and battery mass (equation (2)). Regarding law regulations, to maintain simplicity of the UAV, total mass could not exceed 25 kg. Particular components of mass were estimated according to the following formulas (equations (2) to (5)). The wing mass was calculated according to the empirical formula (equation (3)) from Noth.<sup>18</sup> The fuselage size was defined by the requirement on payload dimensions. Using early CAD model, a wet surface area and fuselage's size were estimated. The surface area multiplied by material weight gave estimation of fuselage mass, which was kept constant. The initial mass of tail booms was estimated according to the same principle as the fuselage mass, based on the early CAD model and assumed material properties. Assuming a unit weight of the two tail booms  $u_{boom}$  equal to 0.32 kg/m, its mass changed depending how far the empennage was situated from the wings and how long the tail booms had to be equation (4). The mass of payload was the design requirement and was constant. All components of avionics like autopilot, sensors, motors, etc. were summed up and also kept constant. From the initial analysis, it was clear that a high total mass of the aircraft is favourable to operate with specified payload, but the design was limited in total mass of 25 kg. Since the total mass of the aircraft was known, the remaining part of the mass could be used for batteries. Transforming equations (equations (2) to (5)) gave mass of batteries. Ultimately, the capacity of the batteries had to be enough to provide at least 1 h of flight endurance

$$m = m_{wing} + m_{fus} + m_{boom} + m_{payload} + m_{avionics} + m_{batt} \quad (2)$$

$$m_{wing} = \frac{5.58 \cdot b^{3.18} \cdot AR^{-0.88}}{g} \quad (3)$$

$$m_{booms} = 2 \cdot l_{boom} \cdot u_{boom} \quad (4)$$

$$m_{batt} = m - (m_{wing} + m_{fus} + m_{boom} + m_{payload} + m_{avionics}) \quad (5)$$

For the dynamic stability analyses, position of center of gravity (CG) and moments of inertia is needed. Change of the position of CG was updated,

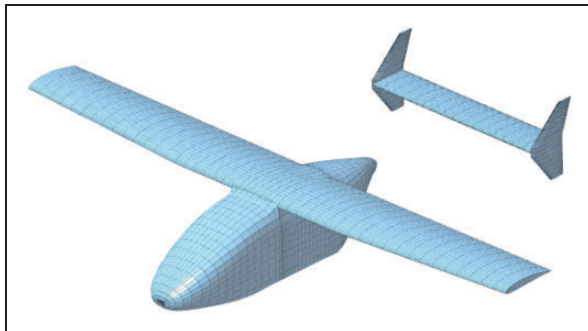


Figure 1. Base aircraft model before the optimization.

due to changing sizes of parts of the structure like for example tail booms. Although, the corrections were small since most of the components of aircraft, with significant masses, were placed fixed inside fuselage and in the tail booms. For keeping the optimization task, simpler moments of inertia were estimated based on the base configuration of the aircraft. Initial calculation of moments of inertia included, besides structure moments of inertia, avionics, payload and propulsion system. Most significant masses, that had high moments of inertia, were not influenced by the optimization variables. Knowing how important moments of inertia can be for the dynamic stability characteristics, the design was updated and analysed again during the detail design phase. The simplification was justified and confirmed in the detail design phase. Nevertheless, improvement for model with changing moments of inertia is desirable and considered as a future work.

### Flight dynamic stability analyses

The flight dynamic stability analyses were done based on data obtained from aerodynamic and mass model simulations. The analyses were done by SDSA software.<sup>19,20</sup> Constraints for the flight dynamic stability for the design are mandatory and defined by the flight law regulations.<sup>21</sup>

### Optimization algorithm

The optimization was done with the use of Particle Swarm Optimization (PSO) algorithm,<sup>22</sup> which belongs to the family of evolutionary algorithms and mimics swarms behaviour. The main equation (6) of the algorithm describes artificial movement of the particles, which represent aircrafts in multiple configurations with different values of design variables, in the design space. Update of the design variable through subsequent iterations is defined by equation (7). The penalty function method was used to incorporate constraints to the optimization

$$\vec{V}_k = w \cdot \vec{V}_{k-1} + s_1 \cdot r_1 \cdot (\vec{x}_{best \text{ in the iteration}} - \vec{x}_k) + s_2 \cdot r_2 \cdot (\vec{x}_{globally \text{ best}} - \vec{x}_k) \quad (6)$$

$$\vec{x}_{k+1} = \vec{x}_k + \vec{V}_k \quad (7)$$

An in-house code algorithm was used.<sup>23,24</sup> Settings of the algorithm are gathered in Table 1. The optimization algorithm was limited to 25 iterations. After about 10 iterations of optimization, improvement of the objective function equation (8) was very small, and it was assumed that the optimization process converged. Optimization task had number of geometrical and environmental variables, which influenced aerodynamics through aircraft's geometry change, flight conditions and mass properties according to

**Table 1.** Optimization algorithm settings.

Settings	
Iterations limit	25
Particles	15
W	0.05
s1	2
s2	2

**Table 2.** List of optimization variables.

Optimization variables			
Id	Name	Min	Max
0	wing_tip_c	0.3	0.5
1	wing_tip_y	1	1.6
2	wing_tip_z	0.225	0.35
3	wing_tip_AoA	0	8
4	h_stab_c	0.2	0.3
5	v_stab_x	1.2	1.5
6	h_stab_AoA	-3.5	3.5
7	v_stab-bot_c	0.05	0.2
8	v_stab-bot_x	0	0.2
9	v_stab-bot_z	0	-0.05
10	v_stab-top_c	0.05	0.2
11	v_stab-top_x	0	0.2
12	v_stab-top_z	0.2	0.32
13	Angle of attack	-3	6
14	AoAmax	6	12
15	wing_AoAcenter	-1	4
16	wing_ccenter	0.3	0.5
17	v_stab-root_c	0.15	0.3
Indexes:	c – chord	x, y, z – positions	

the mass estimation model. All design variables that are listed in Table 2 could change within initially defined, reasonable limits. The limits of the design variables were chosen based on the engineering experience and subsequently tuned if needed during few optimization runs. At the beginning of the optimization process also unfeasible solutions were allowed, but had to be eliminated by the algorithm, during the optimization process, with defined physical constraints. It was assumed that the optimization algorithm should not violate design variables limits, if it is not indicated by the technological, or exploitation issues, to find the true optimum of the solution. It is desirable that only physical constraints are activated by the algorithm during the optimization and lead to the optimum result.

The maximum mass of payload equal to 3 kg and minimum endurance of 1 h were the top-down requirements for the project. From the conceptual phase of the design, it was already known that the

big limiting factor is the total mass of the aircraft ready for flight, which could not exceed 25 kg due to flight law regulations. In such circumstances, it was a challenge to obtain over 1 h of endurance for the electric propulsion. The main objective function was flight endurance equation (8), which was evaluated for the cruise speed of 22 m/s, which was also the top-down condition. The objective function couples all dependencies related to aerodynamics and mass of the aircraft. The design is subject to many constraints. Beginning with basic one where lift force and weight has to be equal in steady flight conditions for cruise speed equation (9). Pitching moment coefficient should be zero equation (10). The stability derivatives should satisfy prescribed values (equations (11) and (12)). The lift distribution should not overcome the prescribed maximum lift coefficient to prevent aerodynamic stall equation (13). The maximum angle of attack (AoA) and related minimum speed were estimated based on the condition during the optimization. Number of additional constraints on wing loading and thrust loading was set (equations (14) to (18)). The conditions for wing loading and thrust loading were estimated during the early conceptual design.

Dynamic stability constraints are defined in the optimization by law regulations and the MIL-STD norms.<sup>25</sup> Constraints on specific, oscillation frequencies, damping ratios and the time to double are prescribed by equations (19) to (24)

Minimize

$$\max_x t(x) = \frac{m_{batt} \cdot k_{batt}}{P} \quad (8)$$

With respect to:

$x$  (design variables; Table 2)

Subject to

$$m \cdot g = \frac{1}{2} \cdot \rho \cdot V^2 \cdot CL \cdot S \quad (9)$$

$$CM|_{CL_{cruise}} = 0 \quad (10)$$

$$\frac{dCL}{dCM} < -0.1 \quad (11)$$

$$\frac{dCn}{d\beta} > 0.004 \quad (12)$$

$$CL_{local\_on\_wing} < 1.4 \quad (13)$$

$$W/S < 0.5 \cdot \rho \cdot V_{min}^2 \cdot CL_{max} \quad (14)$$

$$T/W > \frac{0.5 \cdot \rho \cdot V_{max}^2 \cdot CD_0}{W/S} \quad (15)$$

$$T/W > \sin \gamma + \frac{0.5 \cdot \rho \cdot V_{climb}^2 \cdot CD_0}{W/S}$$

$$+ \frac{W/S}{0.5 \cdot \rho \cdot V_{climb}^2 \cdot \pi \cdot AR \cdot e} \quad (16)$$

$$W/S < \frac{0.5 \cdot \rho \cdot V_{turn}^2 \cdot CL_{max}}{\sqrt{\left(\frac{\theta \cdot V_{turn}}{g}\right)^2 + 1}}$$

where

$$\theta = \frac{g \sqrt{\frac{1}{\cos^2 \varphi} - 1}}{V_{turn}} \quad (17)$$

$$T/W > \frac{0.5 \cdot \rho \cdot V_{turn}^2 \cdot CD_0}{W/S} + \frac{W/S}{\cos^2 \varphi \cdot 0.5 \cdot \rho \cdot V_{turn}^2 \cdot \pi \cdot AR \cdot e} \quad (18)$$

$$\zeta_{phugoid} > 0 \quad (19)$$

$$\zeta_{short\_period} < 1.3 \wedge \zeta_{short\_period} > 0.35 \quad (20)$$

$$\zeta_{dutch\_roll} > 0.19 \quad (21)$$

$$\omega_{dutch\_roll} > 1 \text{ Hz} \quad (22)$$

$$T_{2\_roll} < 1 \text{ s} \quad (23)$$

$$T_{2\_spiral} > 20 \text{ s} \vee T_{2\_spiral} < 0 \text{ s} \quad (24)$$

## Optimization results

The main characteristics of the aircraft obtained after the optimization are shown in Table 3. The total mass of the aircraft for flight was limited to 25 kg. The aircraft requires 374 W of power for flight for cruise conditions. It has the lift to drag ratio equal to 14.3 and is able to achieve flight endurance of about 1 h 40 min. Comparison of geometry layout of the aircraft, before and after optimization, is shown in Figure 2. The most pronouncing change is reduction of the aspect ratio of the wing, which degraded slightly aerodynamic performance, but also reduced mass of the wing. As a consequence, more batteries can be taken, and overall flight endurance increases.

Example of pressure distribution obtained during computations is shown in Figure 3. Because of high

**Table 3.** Chosen properties of the optimized object.

	Result
Wing span (m)	2.4
Mass (kg)	25
Cruise speed (m/s)	22
Cruise required power (W)	374
Aerodynamic efficiency	14.3
Endurance (h)	1.64

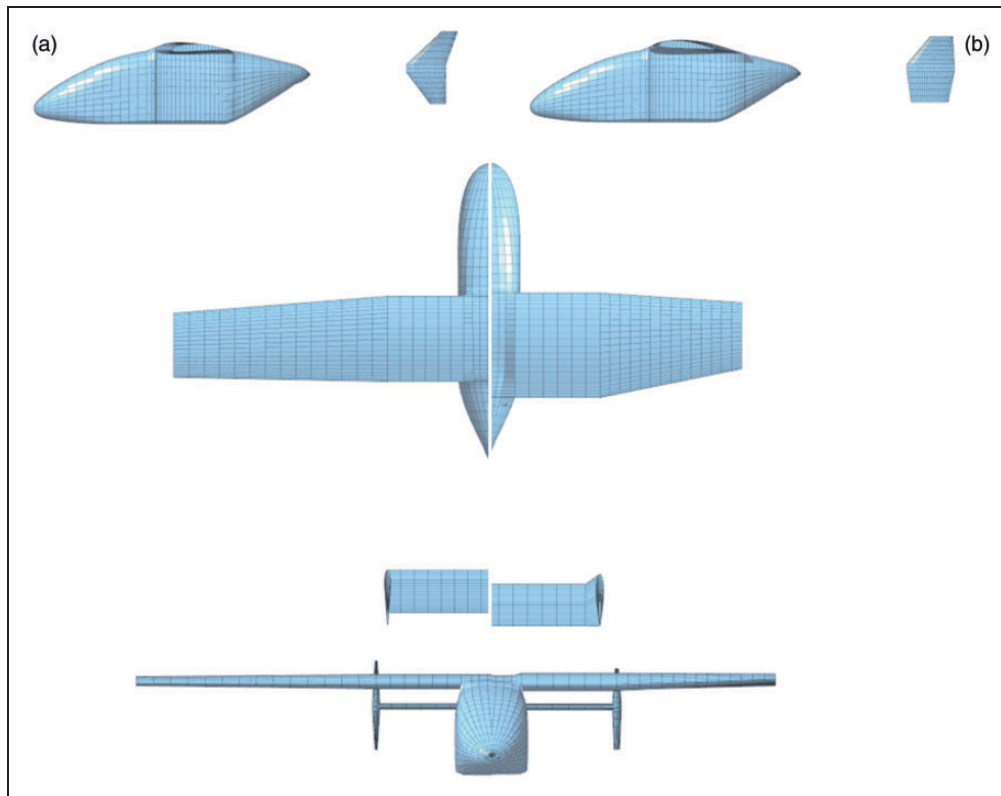


**Figure 2.** Aircraft's geometry comparison: (a) conceptual design configuration and (b) optimized configuration.

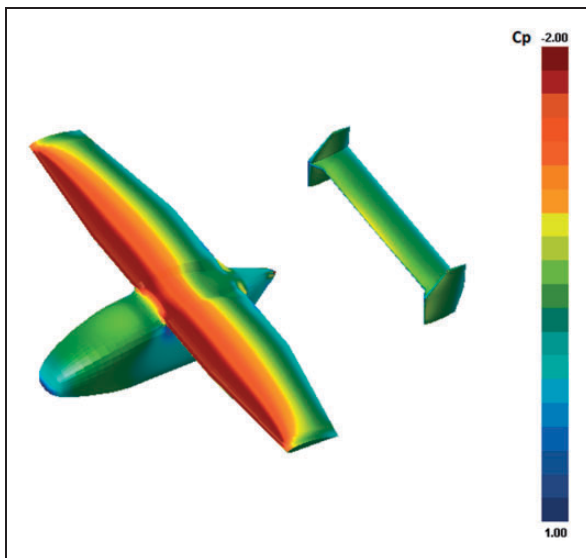


**Figure 3.** Pressure distribution on high angle of attack.

level of computations automation, complexity of the geometry and allowed big changes of the geometry tail booms were not modelled in geometry. It was assumed that their influence on aerodynamics is low compared to other aircraft components, which was confirmed later on in more complex verification computations. Still mass of the tail booms was dependable on their length equation (4). Total mass break down is shown in Table 4.

**Table 4.** Mass brake down of the aircraft in kilograms.

	Optimal
m_wing	2.21
m_fuselage	3.8
m_booms	1.13
m_payload	3
m_const	9.26
m_batt	5.6
m	25

As stated before, optimization process was subject to many constraints, which had to be satisfied. The constraints were realized by penalty function method, and in the end, only four constraints were slightly violated, which had to be carefully checked (Figure 4). Lift force and weight equality constraint gave difference of 0.21 kg, which is 0.8% of the total weight and is considered as a good result within tolerance. Pitching moment coefficient in trim conditions should be zero, and after the optimization, it had the value of  $-0.0018$ . This is also considered as satisfactory, and in practice, this difference can be corrected by a small elevator deflection. Local lift coefficients were crossed, which could lead to undesirable stall conditions. This important constraint on the local lift coefficient had set safety margin in the optimization. Figure 5 shows



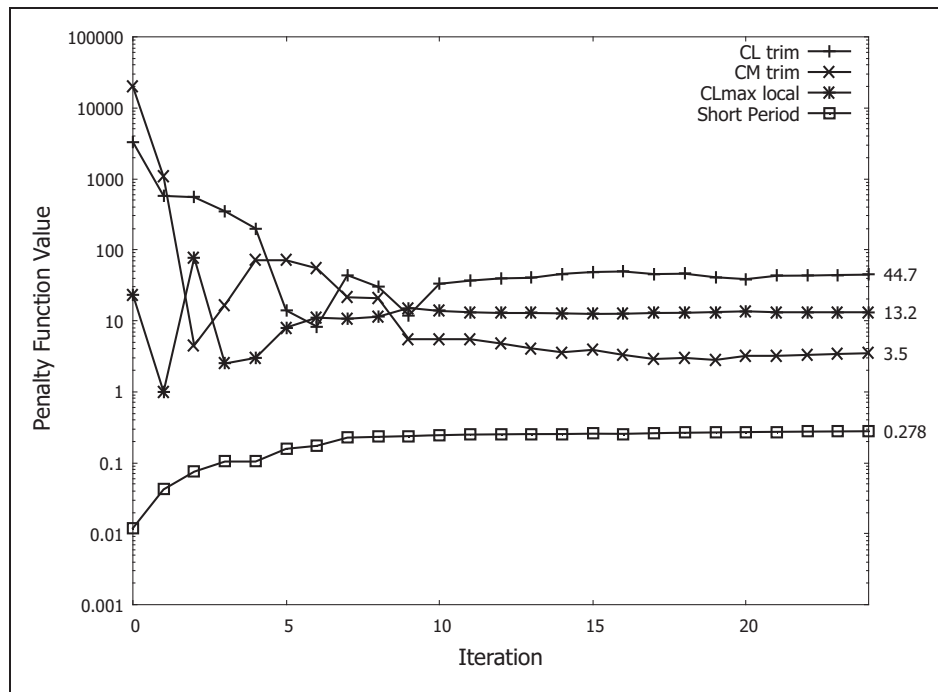


**Figure 4.** Penalty function of the constraints through the optimization.

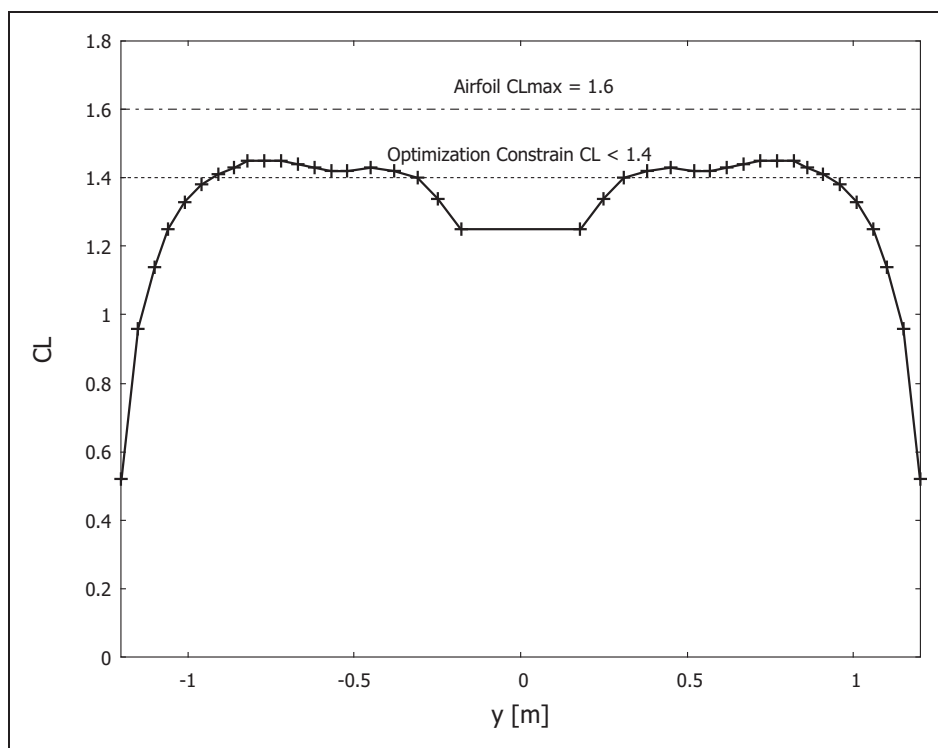


**Figure 5.** Lift distribution on the wing.

the lift distribution with optimization constraint and maximum airfoil lift coefficient marked. The constraint was only slightly violated, and maximum lift coefficient for the airfoil used is clearly higher, which indicates that the design still remains on the safe side.

Finally, the dynamic stability short period constrain was very slightly violated. This constrain is discussed in detail during the dynamic stability characteristics description. All other modes of the dynamic stability were fully satisfied.

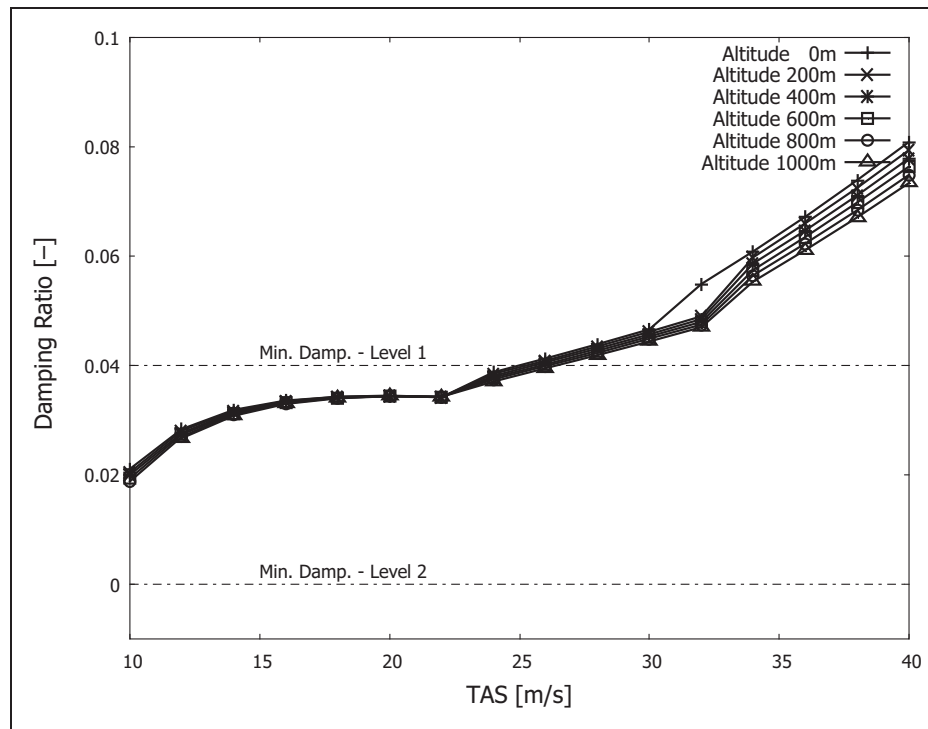


Figure 6. Phugoid mode – damping ratio.

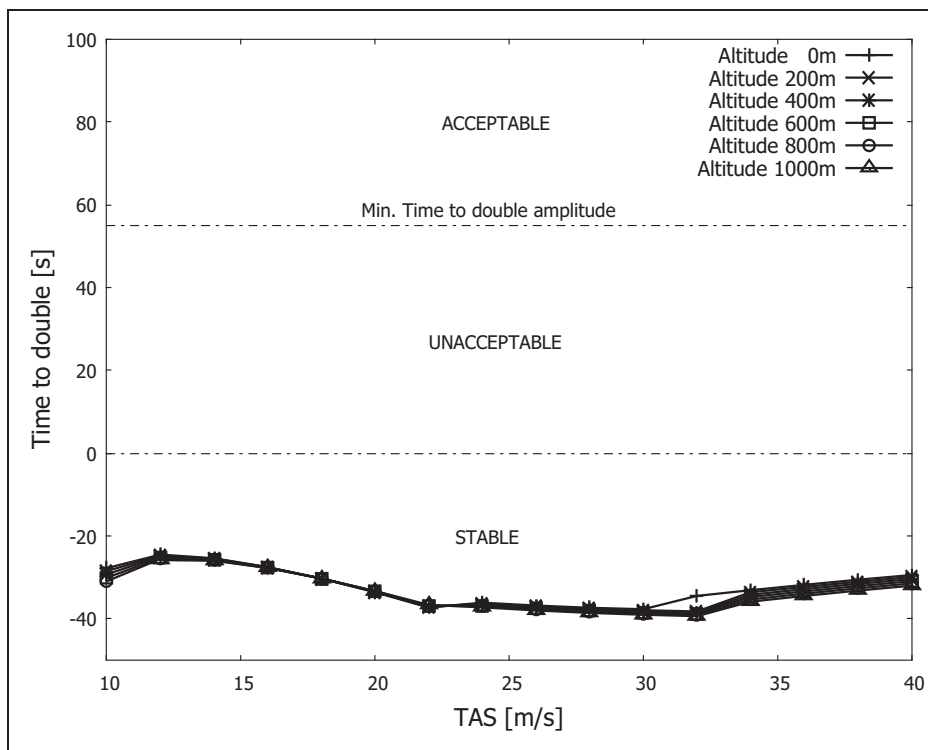


Figure 7. Time to double for phugoid.

### Flight dynamic stability optimization constraints

The optimization is constrained, by flight law regulations described in the following work,<sup>21</sup> to certain aircraft stability properties. All stability modes were

stable for all needed flight speeds and altitudes. Results of the analyses are shown in the following part.

More precise requirements from MIL<sup>25</sup> criteria define phugoid damping ratios. Obtained damping characteristics are satisfied through the whole range

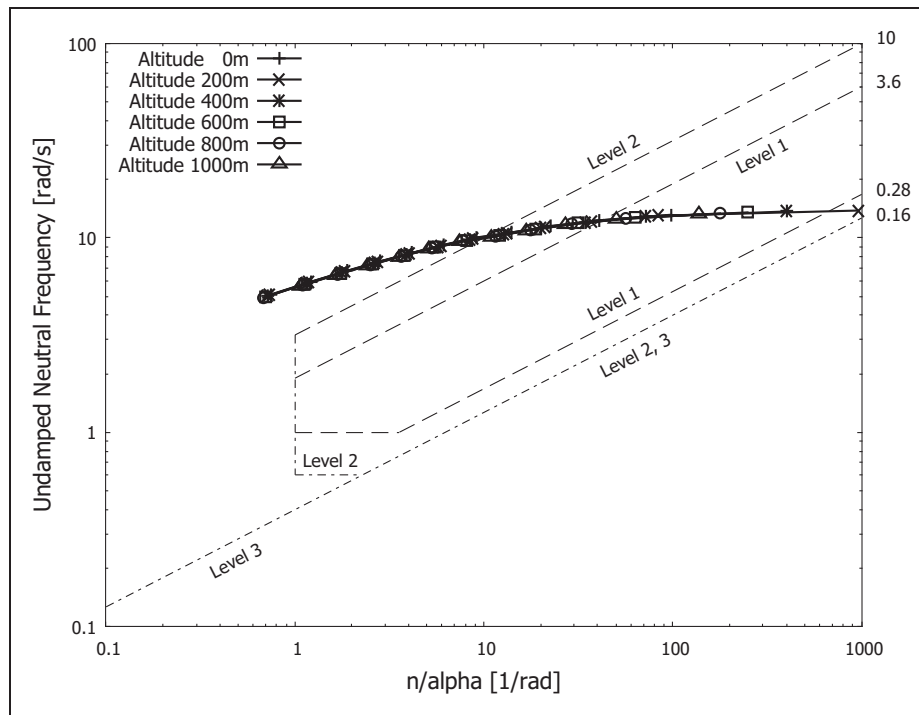


Figure 8. Short period – control anticipation parameter (CAP) requirement.

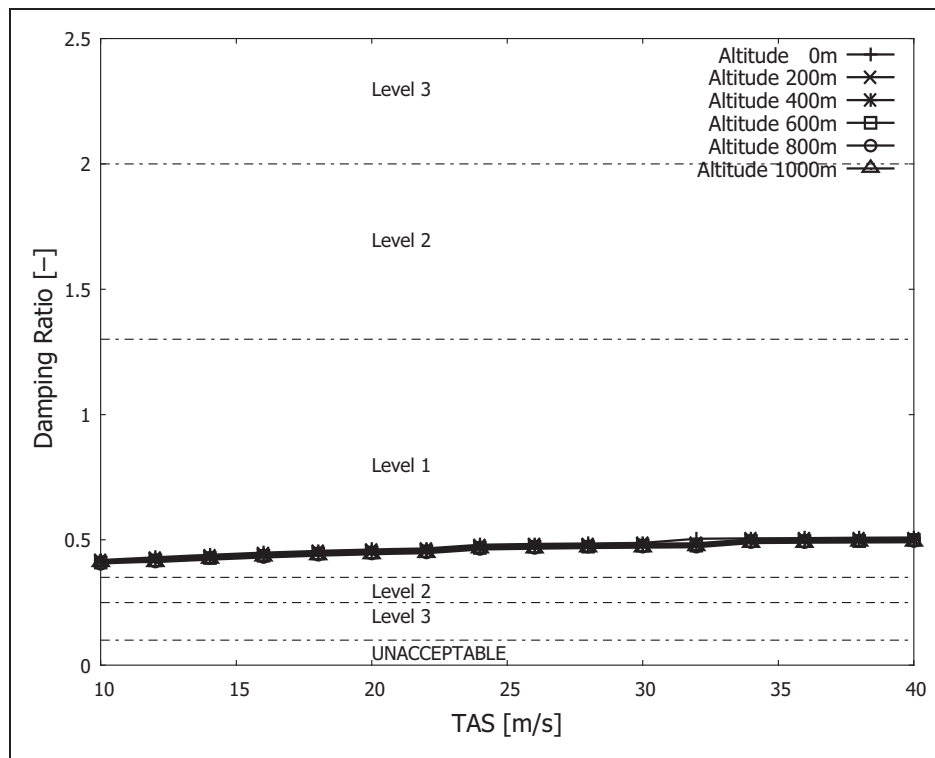


Figure 9. Short period mode – damping ratio.

of airspeeds and altitudes. Only for regime of low speeds, the damping ratios exceed slightly Level 2 of acceptance, see Figure 6. Values of phugoid the time to double are negative, which indicates that the oscillations are stable at all times, see Figure 7.

Short period gives strict requirements for oscillations which have to be strongly damped, what is emphasized in flight regulations as well as in MIL requirements. The short period undamped natural frequency is shown in Figure 8. The short period



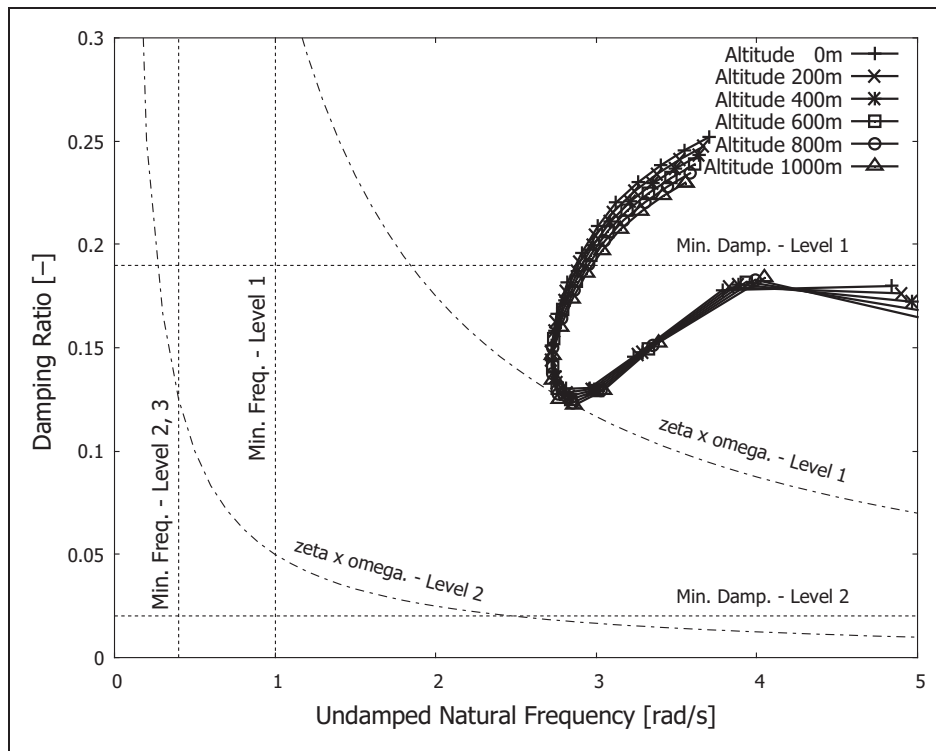


Figure 10. Dutch roll for flight phase C characteristics.

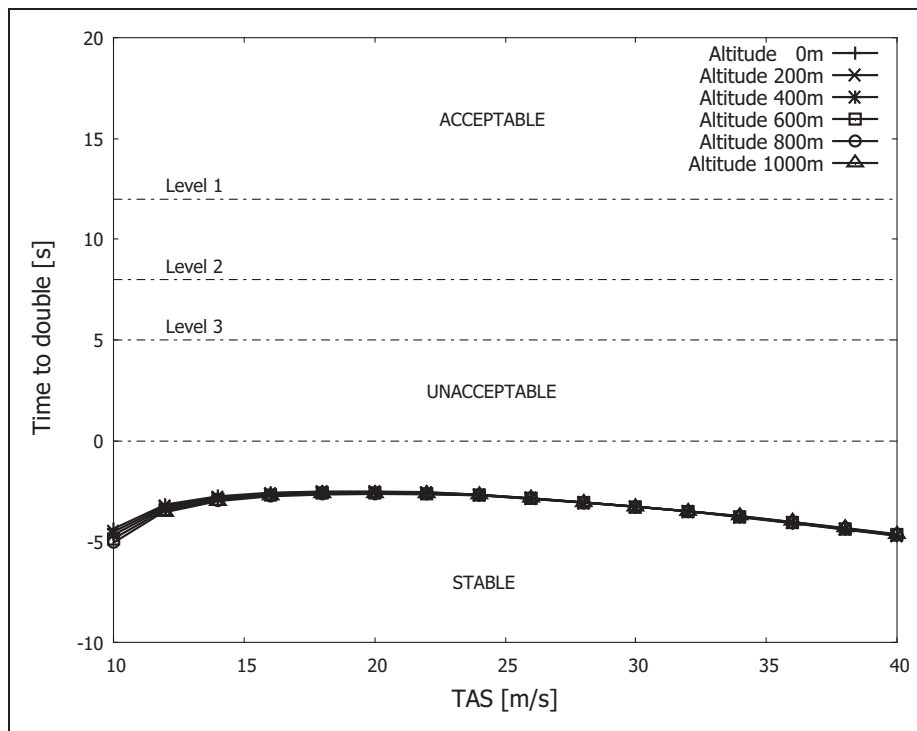


Figure 11. Spiral mode – time to double.

frequencies are partially in the second acceptance level of MIL norms, but they are still satisfactory. Damping ratio of the short period is given in Figure 9. The characteristics fall into the first acceptance level of the flight regulations and are strongly damped.

Dutch roll characteristics are shown in Figure 10 for flight phase C. Takeoff and landing are covered during that phase of flight, which are one of the most dangerous phases and have to be treated carefully. The conditions are fulfilled.

Constraints for the spiral mode are shown in Figure 11. At all times, the spiral is stable, what is indicated by a negative time to double values.

## Conclusion

This work presents optimization framework of coupling aerodynamic analyses, mass analyses and flight dynamic constraints. It was presented how aerodynamic analyses were done, and how mass models of components of the aircraft were defined. It was also shown what kind of optimization algorithm was used for this design, and how the optimization task was defined. A special attention was paid to the constraints which were slightly violated and presented in this article, that with the design assumptions made, the constraints remain satisfied. Finally, all crucial dynamic stability characteristics were presented and shown that they all are on the right acceptance level.

All constraints are satisfied and the goal of the optimization achieved, which is stable aircraft with a very good performance. Detailed approach of defining and solving the optimization task was shown in this article. The optimization process is fully automated resulting in a mature preliminary design.

It was proved that the optimization framework, which utilizes in the design process constraints from the flight dynamic longitudinal and lateral stability, is robust and feasible.

## Declaration of Conflicting Interests

The author(s) declared no potential conflicts of interest with respect to the research, authorship, and/or publication of this article.

## Funding

The author(s) disclosed receipt of the following financial support for the research, authorship, and/or publication of this article: EU funds under the Smart Growth Operational Program 2014-2020, Polish Project No.: POIR.01.01.01-00-0814/17

## ORCID iD

Jacek Mieloszyk  <https://orcid.org/0000-0002-4446-7919>

## References

1. Benaouali A and Kachel S. A surrogate-based integrated framework for the aerodynamic design optimization of a subsonic wing planform shape. *Proc IMechE, Part G: J Aerospace Engineering*. Epub ahead of print 22 March 2017. DOI: 10.1177/0954410017699007.
2. Benaouali A and Kachel S. Multidisciplinary design optimization of aircraft wing using commercial software. *Integr Aerosp Sci Technol* 2019; 92: 766–776.
3. Figat M and Kwiek A. Aerodynamic optimisation of the rocket plane in subsonic and supersonic flight conditions. *J Aerosp Eng*. Epub ahead of print 14 August 2017. DOI: 10.1177/0954410017723672.
4. Klimczyk W and Goraj Z. Analysis and optimization of morphing wing aerodynamics. *Aircr Eng Aerosp Technol* 2019; 91: 538–546.
5. Klimczyk W and Goraj Z. Robust design and optimization of UAV empennage. *Aircr Eng Aerosp Technol* 2017; 89: 609–619.
6. Bazile MJ and Calderara MF. Aircraft dynamic lateral stability analytic formulation for Dutch roll mode stability prediction. *Prog Flight Phys* 2012; 3: 53–62.
7. Bras M, Vale J, Lau F, et al. Flight dynamics and control of a vertical tailless aircraft. *Aeronaut Aerosp Eng*. Epub ahead of print January 2013. DOI: 10.4172/2168-9792.1000119.
8. Mader ChA and Martins JRRA. Stability-constrained aerodynamic shape optimization of flying wings. *J Aircr* 2013; 50: 1431–1449.
9. Morris CC, Sultan C, Allison DL, et al. Towards flying qualities constraints in the multidisciplinary design optimization of a supersonic tailless aircraft. In: *12th AIAA aviation technology, integration, and operations (ATIO) conference and 14th AIAA/ISSM*, 17–19 September 2012, Indianapolis, IN, USA.
10. Goetzendorf-Grabowski T and Rodzewicz M. Design of UAV for photogrammetric mission in Antarctic area aerodynamic and stability analysis of personal vehicle in tandem-wing configuration. *J Aerosp Eng* 2016; 231: 1660–1675.
11. Goetzendorf-Grabowski T and Antoniewski T. Three surface aircraft (TSA) configuration – flying qualities evaluation. *Aircr Eng Aerosp Technol* 2016; 88: 277–284.
12. Goraj Z. Flight dynamics models used in different national and international projects. *Aircr Eng Aerosp Technol Int J* 2014; 86: 166–178.
13. Mieloszyk J and Goetzendorf-Grabowski T. Introduction of full flight dynamic stability constraints in aircraft multidisciplinary optimization. *Aerosp Sci Technol* 2017; 68: 252–260.
14. Goetzendorf-Grabowski T. Multi-disciplinary optimization in aeronautical engineering. *J Aerosp Eng* 2017; 231: 2305–2313.
15. Goetzendorf-Grabowski T and Mieloszyk J. Common computational model for coupling panel method with finite element method. *Aircr Eng Aerosp Technol* 2017; 89: 654–662.
16. Drela M. XFOIL: an analysis and design system for low Reynolds number airfoils. In: Mueller TJ (ed) *Low Reynolds number aerodynamics*. Lecture Notes in Engineering. vol. 54, 1989, pp.1–12. Berlin, Germany: Springer.
17. Gudmundsson S. *General aviation aircraft design: applied methods and procedures*. 1st ed. Amsterdam, The Netherlands: Elsevier Inc., 2014.
18. Noth A. *Design of solar powered airplanes for continuous flight*. Doctoral Thesis, ETH Zurich, 2008.
19. Goetzendorf-Grabowski T. SDSA – simulation and dynamic stability analysis – software package. Warsaw University of Technology, [www.meil.pw.edu.pl/add/ADD/Teaching/Software/SDSA](http://www.meil.pw.edu.pl/add/ADD/Teaching/Software/SDSA) (2018, accessed 10 May 2020).
20. Goetzendorf-Grabowski T, Miesalski D and Marcinkiewicz E. Stability analysis using SDSA tool. *Prog Aerosp Sci* 2011; 47: 636–646.

21. European Aviation Safety Agency Certification Specifications for Normal, Utility, Aerobatic, and Commuter Category Aeroplanes – CS-23, Amendment 3, 2012.
22. Kennedy J and Eberhart R. Particle swarm optimization. In: *Proceedings of the IEEE international conference on neural networks*, Perth, Australia, 1995, pp.1942–1945.
23. Mieloszyk J. Handling optimization problems on an example of micro UAV. In: *Proceedings of the 3rd CEAS air & space conference, 21st AIDAA congress*, Venice, Italy, 24–28 October 2011.
24. Mieloszyk J. OptiM – software package for numerical optimization, Warsaw University of Technology, [www.meil.pw.edu.pl/add/ADD/Teaching/Software/OptiM](http://www.meil.pw.edu.pl/add/ADD/Teaching/Software/OptiM) (2018, accessed 10 May 2020).
25. MIL-F-8785C – Military specification flying qualities of piloted airplanes, 5 November 1980.

## Appendix

### Notation

$AR$	aspect ratio
$CD$	aerodynamic drag coefficient
$CL$	aerodynamic lift coefficient
$CM$	aerodynamic moment coefficient
$D$	aerodynamic drag (N)
$e$	Oswald coefficient

$g$	gravity acceleration, 9.81 (m/s <sup>2</sup> )
$k_{batt}$	power density in batteries (W/kg)
$l$	geometry dimension, length (m)
$m$	mass (kg)
$P$	power (W)
$r_1, r_2$	randomization coefficients in PSO optimization algorithm
$s_1, s_2$	relaxation coefficients in PSO optimization algorithm
$S$	reference area (m <sup>2</sup> )
$t$	flight endurance (s)
$T$	thrust (N)
$T_2$	time to double (s)
$u_{boom}$	unit mass of the tail boom 0.32 (kg/m)
$w$	global relaxation coefficients in PSO optimization algorithm
$W$	weight (N)
$V$	flight velocity (m/s)
$V_k$	particles velocity vector in optimization
$x$	optimization design variables
$\beta$	sideslip angle
$\gamma$	climb angle
$\varphi$	roll angle
$\rho$	air density (kg/m <sup>3</sup> )
$\omega$	frequency of oscillations (Hz)
$\zeta$	damping ratio